

# Structural Information through NMR Hyperfine Shifts in Blue Copper Proteins

Ivano Bertini,<sup>\*,†</sup> Claudio O. Fernández,<sup>‡,§</sup> B. Göran Karlsson,<sup>||</sup> Johan Leckner,<sup>||</sup> Claudio Luchinat,<sup>†</sup> Bo G. Malmström,<sup>⊥</sup> Aram M. Nersissian,<sup>#</sup> Roberta Pierattelli,<sup>†</sup> Eric Shipp,<sup>#</sup> Joan S. Valentine,<sup>#</sup> and Alejandro J. Vila<sup>§,§</sup>

Contribution from the Magnetic Resonance Center, University of Florence, Via Luigi Sacconi 6, 50019 Sesto Fiorentino, Florence, Italy, LANAIS RMN-300, Facultad de Farmacia y Bioquímica, Universidad de Buenos Aires, Junín 956, 1113 Buenos Aires, Argentina, Department of Molecular Biotechnology, Chalmers University of Technology, P.O. Box 462 SE-405 30 Göteborg, Sweden, Department of Chemistry, Biochemistry and Biophysics, Göteborg University, SE-40530 Göteborg, Sweden, Department of Chemistry and Biochemistry, University of California, Los Angeles, California 90095, and Area Biofisica, Facultad de Ciencias Bioquímicas y Farmacéuticas, Universidad Nacional De Rosario, Suipacha 531, 2000 Rosario, Argentina

Received July 28, 1999. Revised Manuscript Received November 4, 1999

**Abstract:** The oxidized blue copper proteins azurin and stellacyanin have been investigated through <sup>1</sup>H NMR at 800 MHz and the results compared with those for plastocyanin (Bertini, I.; Ciurli, S.; Dikiy, A.; Gasanov, R.; Luchinat, C.; Martini, G.; Safarov, N. *J. Am. Chem. Soc.* **1999**, *121*, 2037). By exploiting saturation transfer between the oxidized and the reduced forms, all the hyperfine shifted signals can be assigned, including the β-CH<sub>2</sub> protons of the coordinated cysteines, which are so broad not to be detected under direct observation. Both hyperfine shifts and line widths of the latter signals differ dramatically from one protein to another: average hyperfine shifts of about 850, 600, and 400 ppm and average line widths of 1.2, 0.45, and 0.25 MHz are observed for azurin, plastocyanin, and stellacyanin, in that order. The observation of a nuclear line width of 1.2 MHz is unprecedented in high-resolution NMR in solution. These data are interpreted as a measure of the out-of-plane displacement of the copper ion, which increases on passing from azurin to plastocyanin to stellacyanin. The present approach seems general for the investigation of blue copper proteins.

## Introduction

Electron transfer in metalloproteins is regulated by the environment of the metal center.<sup>1,2</sup> The polypeptide matrix plays an important role in determining the electronic structure of the metal site as well as the efficiency of the intervening medium in long-range electron transfer. Magnetic spectroscopies have been widely applied to the characterization of electron-transfer proteins, since at least one of the redox states is paramagnetic. Among them, NMR has played a key role in defining details of the electronic structures of these systems. Cytochromes,<sup>3–5</sup> as well as iron–sulfur proteins,<sup>6</sup> have been thoroughly studied by paramagnetic NMR. This has not been

the case for copper proteins. The slow electronic relaxation rates of copper(II) ions<sup>7,8</sup> have precluded NMR investigations of protons belonging to the donor groups because the lines are broad beyond detectable limits. For that reason, cobalt(II)<sup>9–19</sup> and nickel(II)<sup>20–23</sup> substituted derivatives of copper proteins

\* Author to whom correspondence should be addressed: (Tel) +39 055 4209272; (fax) +39 055 4209271; (e-mail) bertini@cerm.unifi.it.

† University of Florence.

‡ Universidad de Buenos Aires.

§ Staff member of CONICET (Argentina).

|| Chalmers University of Technology.

⊥ Göteborg University.

• Deceased February 9, 2000.

# University of California.

§ Universidad Nacional de Rosario.

- (1) Gray, H. B.; Winkler, J. R. *Annu. Rev. Biochem.* **1996**, *65*, 537–561.
- (2) Winkler, J. R.; Wittung, P.; Leckner, J.; Malmström, B. G.; Gray, H. B. *Proc. Natl. Acad. Sci. U.S.A.* **1997**, *94*, 4246–4249.
- (3) Bertini, I.; Turano, P.; Vila, A. J. *Chem. Rev.* **1993**, *93*, 2833–2932.
- (4) Banci, L.; Bertini, I.; Luchinat, C.; Turano, P. In *The Porphyrin Handbook*; Kadish, K. M., Smith, K. M., Guilard, R., Eds.; Academic Press: Burlington, MA, 1999 and references therein.
- (5) Shokhirev, N. V.; Walker, F. A. *JBIC, J. Biol. Inorg. Chem.* **1998**, *3*, 581–594.

- (6) Bertini, I.; Luchinat, C.; Rosato, A. In *Advances in Inorganic Chemistry*; Sykes, A. G., Cammack, R., Eds.; Academic Press: San Diego, 1999; pp 251–282 and references therein.
- (7) Bertini, I.; Briganti, F.; Luchinat, C.; Mancini, M.; Spina, G. *J. Magn. Reson.* **1985**, *63*, 41–55.
- (8) Banci, L.; Bertini, I.; Hallewell, R. A.; Luchinat, C.; Viezzoli, M. S. *Eur. J. Biochem.* **1989**, *184*, 125–129.
- (9) Hill, H. A. O.; Storm, C. B.; Ambler, R. P. *Biochem. Biophys. Res. Commun.* **1976**, *70*, 783–790.
- (10) Moratal Mascarell, J. M.; Salgado, J.; Donaire, A.; Jimenez, H. R.; Castells, J. *Inorg. Chem.* **1993**, *32*, 3587–3588.
- (11) Vila, A. J. *FEBS Lett.* **1994**, *355*, 15–18.
- (12) Vila, A. J.; Fernández, C. O. *J. Am. Chem. Soc.* **1996**, *118*, 7291–7298.
- (13) Piccioli, M.; Luchinat, C.; Mizoguchi, T. J.; Ramirez, B. E.; Gray, H. B.; Richards, J. H. *Inorg. Chem.* **1995**, *34*, 737–742.
- (14) Salgado, J.; Jimenez, H. R.; Donaire, A.; Moratal, J. M. *Eur. J. Biochem.* **1995**, *231*, 358–369.
- (15) Salgado, J.; Jimenez, H. R.; Moratal Mascarell, J. M.; Kroes, S. J.; Warmerdam, G. C. M.; Canters, G. W. *Biochemistry* **1996**, *35*, 1810–1819.
- (16) Fernández, C. O.; Sannazzaro, A. I.; Vila, A. J. *Biochemistry* **1997**, *36*, 10566–10570.
- (17) Vila, A. J.; Ramirez, B. E.; Di Bilio, A. J.; Mizoguchi, T. J.; Richards, J. H.; Gray, H. B. *Inorg. Chem.* **1997**, *36*, 4567–4570.
- (18) Donaire, A.; Salgado, J.; Moratal, J. M. *Biochemistry* **1998**, *37*, 8659–8673.
- (19) Salgado, J.; Kroes, S. J.; Berg, A.; Moratal Mascarell, J. M.; Canters, G. W. *J. Biol. Chem.* **1998**, *273*, 177–185.

have frequently been used for characterization of the metal ligand set by NMR, as well as to retrieve information on the electronic structure of naturally occurring and mutated blue copper sites.

Blue copper proteins (BCPs) possess rigid copper-binding sites<sup>24–31</sup> designed for efficient electron transfer by minimization of reorganization effects upon changes in the oxidation state.<sup>32</sup> The coordination geometry gives rise to low-lying electronic excited states that make the electronic relaxation rates 1 order of magnitude faster than in tetragonal Cu(II) complexes.<sup>33</sup> This finding has allowed several groups to record NMR spectra of BCPs in their oxidized state,<sup>16,17,19,34</sup> after the initial report from Kalverda et al.<sup>35</sup> However, only partial assignments have been achieved to date. Bertini et al. have recently shown that all NMR signals corresponding to metal ligands of plastocyanin in its Cu(II) form can be assigned by performing saturation transfer experiments in a sample containing a nearly 1:1 ratio of oxidized and reduced forms of the protein.<sup>36</sup> These experiments rely on the fact that the electron self-exchange rate between the two redox states in equilibrium is of the right order of magnitude to allow transfer of magnetization between a nucleus in the oxidized species and the same nucleus in the reduced species, when the former is subjected to continuous wave irradiation in a 1D NMR experiment. The novelty of this approach resides in the fact that this strategy can be applied to locate the spectral position of NMR signals far away and broadened beyond detectable limits in the oxidized form. This strategy is particularly useful for blue copper centers since it allows detection of signals of the Cys residue coordinated to copper.

The spectroscopic features of blue copper sites in the oxidized state are largely dominated by the strong Cu(II)–Cys interaction, which is controlled by an unusual coordination geometry imposed by the protein scaffolding.<sup>28,30,37</sup> The electronic spectra in the visible range show intense absorption bands around 600 and 450 nm assigned as ligand-to-metal charge-transfer bands, reflecting the large overlap between the Cu  $d_{x^2-y^2}$  and the sulfur orbitals.<sup>38–44</sup> EPR spectra of BCPs are also characteristic in exhibiting small  $A_{||}$  values.<sup>38</sup> The resulting high anisotropic

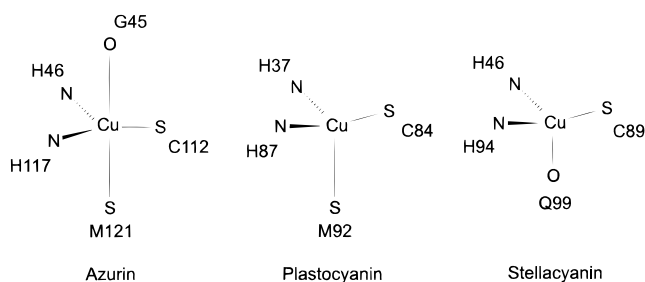


**Figure 1.** Schematic drawing of the active site of *P. aeruginosa* azurin, spinach plastocyanin, and cucumber stellacyanin.

covalency in the metal centers would favor the electron transfer along the Cu–S bond through a superexchange mechanism.<sup>30,37</sup> Theoretical calculations<sup>40,41</sup> and XAS<sup>42</sup> and ENDOR<sup>45</sup> measurements have supported this view, and the recent NMR data on plastocyanin have confirmed the existence of a large extent of electron delocalization onto the bound Cys.<sup>36</sup>

The general copper-binding motif in BCPs exhibits some variations between different proteins.<sup>25,31</sup> The copper ion is bound to a Cys sulfur and two His nitrogens that lie approximately in the same plane while the nature and the degree of interaction with the axial ligand appear to be responsible for tuning the properties of the metal site.<sup>30,37,44,46</sup> In most BCPs, a Met residue is the axial ligand, generally exhibiting a weak binding, with Cu–Sδ distances ranging from 2.6 to 3.0 Å.<sup>25,31</sup> After the investigation of plastocyanin,<sup>36</sup> which has an axial methionine ligand, we decided to extend the NMR hyperfine investigation to two other BCPs with different extents of perturbation induced by the axial ligands, namely, azurin from *Pseudomonas aeruginosa*, and cucumber stellacyanin. The former has a weakly bound methionine and a peptide carbonyl as axial ligands, and the latter has a more strongly bound glutamine, as schematically shown in Figure 1.

## Experimental Section

**Protein Expression and Purification.** *P. aeruginosa* azurin was expressed and purified as previously described.<sup>47</sup> NMR samples (~5 mM) were prepared in D<sub>2</sub>O or H<sub>2</sub>O (plus 5% D<sub>2</sub>O for the lock), in 10 mM phosphate buffer, at both pH 5.0 and 8.0. Solutions in D<sub>2</sub>O were obtained by solvent exchange using Pall Filtrun Nanosep centrifugal microconcentrators.

Cucumber stellacyanin was purified as previously described.<sup>48</sup> NMR samples (~7 mM) were prepared in D<sub>2</sub>O or H<sub>2</sub>O (plus 5% D<sub>2</sub>O for the lock), in 50 mM phosphate buffer, at pH 6.0 and 7.0. Solutions in

(20) Blaszk, J. A.; Ulrich, E. L.; Markley, J. L.; McMillin, D. R. *Biochemistry* **1982**, *21*, 6253–6258.

(21) Moratal Mascarell, J. M.; Salgado, J.; Donaire, A.; Jimenez, H. R.; Castells, J. *J. Chem. Soc., Chem. Commun.* **1993**, 110–112.

(22) Moratal Mascarell, J. M.; Salgado, J.; Donaire, A.; Jimenez, H. R.; Castells, J.; Martinez Ferrer, M. *J. Magn. Reson. Chem.* **1993**, *31*, S41–S46.

(23) Fernández, C. O.; Sannazzaro, A. I.; Vila, A. *J. Inorg. Chim. Acta* **1998**, *273*, 367–371.

(24) Nar, H.; Messerschmidt, A.; Huber, R.; van de Kamp, M.; Canters, G. W. *J. Mol. Biol.* **1991**, *221*, 765–772.

(25) Adman, E. T. *Adv. Protein Chem.* **1991**, *42*, 144–197.

(26) Sykes, A. G. *Adv. Inorg. Chem.* **1991**, *30*, 7–408.

(27) Guss, J. M.; Bartunik, H. D.; Freeman, H. C. *Acta Crystallogr.* **1992**, *B48*, 790–811.

(28) Malmström, B. G. *Eur. J. Biochem.* **1994**, *223*, 711–718.

(29) Hart, J. P.; Nersissian, A. M.; Herrmann, R. G.; Nalbandyan, R. M.; Valentine, J. S.; Eisenberg, D. *Protein Sci.* **1996**, *5*, 2175–2183.

(30) Solomon, E. I.; Penfield, K. W.; Gewirth, A. A.; Lowery, M. D.; Shadle, S. E.; Guckert, J. A.; LaCroix, L. B. *Inorg. Chim. Acta* **1996**, *243*, 67–78.

(31) Messerschmidt, A. *Struct. Bonding* **1998**, *90*, 37–68.

(32) Di Bilio, A. J.; Hill, M. G.; Bonander, N.; Karlsson, B. G.; Villahermosa, R. M.; Malmström, B. G.; Winkler, J. R.; Gray, H. B. *J. Am. Chem. Soc.* **1997**, *119*, 9921–9922.

(33) Kroes, S. J.; Salgado, J.; Parigi, G.; Luchinat, C.; Canters, G. W. *JBIC, J. Biol. Inorg. Chem.* **1996**, *1*, 551–559.

(34) Dennison, C.; Kohzuma, T. *Inorg. Chem.* **1999**, *38*, 1491–1497.

(35) Kalverda, A. P.; Salgado, J.; Dennison, C.; Canters, G. W. *Biochemistry* **1996**, *35*, 3085–3092.

(36) Bertini, I.; Ciurli, S.; Dikiy, A.; Gasanov, R.; Luchinat, C.; Martini, G.; Safarov, N. *J. Am. Chem. Soc.* **1999**, *121*, 2037–2046.

(37) Holm, R. H.; Kennepohl, P.; Solomon, E. I. *Chem. Rev.* **1996**, *96*, 2239–2314.

(38) Malmström, B. G.; Vänngård, T. *J. Mol. Biol.* **1960**, *2*, 118–124.

(39) Gray, H. B.; Solomon, E. I. In *Copper Proteins*; Spiro, T. G., Ed.; Wiley: New York, 1981; pp 1–39.

(40) Penfield, K. W.; Gewirth, A. A.; Solomon, E. I. *J. Am. Chem. Soc.* **1985**, *107*, 4519–4529.

(41) Gewirth, A. A.; Solomon, E. I. *J. Am. Chem. Soc.* **1988**, *110*, 3811–3819.

(42) George, S. J.; Lowery, M. D.; Solomon, E. I.; Cramer, W. A. *J. Am. Chem. Soc.* **1993**, *115*, 2968–2969.

(43) Lu, Y.; LaCroix, L. B.; Lowery, M. D.; Solomon, E. I.; Bender, C. J.; Peisach, J.; Roe, J. A.; Gralla, E. B.; Valentine, J. S. *J. Am. Chem. Soc.* **1993**, *115*, 5907–5918.

(44) Andrew, C. R.; Yeom, H.; Valentine, J. S.; Karlsson, B. G.; Bonander, N.; van Pouderoyen, G.; Canters, G. W.; Loehr, J. S.; Sanders-Loehr, J. *J. Am. Chem. Soc.* **1994**, *116*, 11489–11498.

(45) Werst, M. M.; Davoust, E. E.; Hoffman, B. M. *J. Am. Chem. Soc.* **1991**, *113*, 1533–1538.

(46) Wittung-Stafshede, P.; Hill, M. G.; Gomez, E.; Di Bilio, A. J.; Karlsson, B. G.; Leckner, J.; Winkler, J. R.; Gray, H. B.; Malmström, B. G. *JBIC, J. Biol. Inorg. Chem.* **1998**, *3*, 367–370.

(47) Karlsson, B. G.; Pascher, T.; Nordling, M.; Arvidsson, R. H.; Lundberg, L. G. *FEBS Lett.* **1989**, *236*, 211–217.

(48) Nersissian, A. M.; Mehrabian, Z. B.; Nalbandyan, R. M.; Hart, J. P.; Fraczkiwicz, G.; Czernuszawicz, R. S.; Bender, C. J.; Peisach, J.; Herrmann, R. G.; Valentine, J. S. *Protein Sci.* **1996**, *5*, 2184–2192.

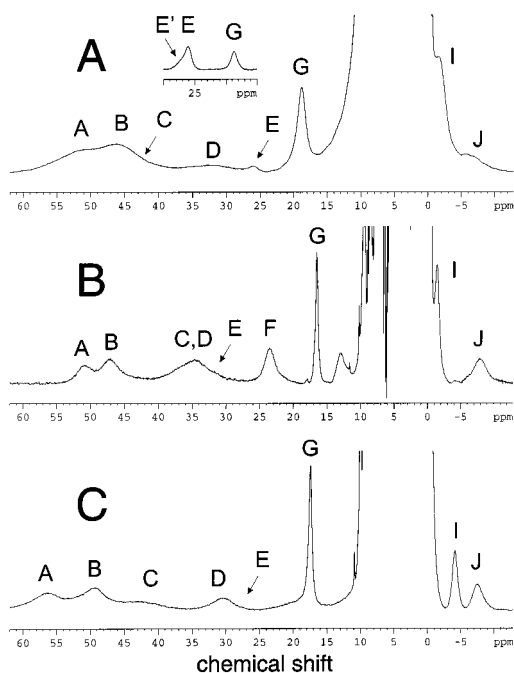


**Figure 2.**  $^1\text{H}$  NMR 800 MHz spectra of oxidized (A) *P. aeruginosa* azurin, (B) spinach plastocyanin, and (C) cucumber stellacyanin recorded at 298 K in  $\text{D}_2\text{O}$  solution. Residual exchangeable signals are indicated with arrows. In the inset of panel A, a portion of the spectrum recorded in  $\text{H}_2\text{O}$  solution is reported.

$\text{D}_2\text{O}$  were obtained by solvent exchange utilizing an ultrafiltration Centricon cell.

In all cases, sodium ascorbate solubilized in the proper buffer was added to the samples in order to reach a 1:1 ratio between oxidized and reduced forms in solution.

**NMR Spectroscopy.** The NMR spectra were recorded on a Bruker Avance 800 spectrometer operating at proton frequencies of 800.13 MHz using a standard TXI probe head. The reported pH values in  $\text{D}_2\text{O}$  solutions are not corrected for the deuterium isotope effect. All chemical shifts were referenced to the chemical shift of the residual HDO signal, which was calibrated against external DSS.

1D spectra were acquired by using the superWEFT pulse sequence<sup>49</sup> or by using the 1–3–3–1 water suppression scheme.<sup>50</sup> Typical repetition rates were in the range 100–200 ms.

Saturation transfer experiments were performed using an “on–off” scheme where “on” values were varied from 10 to 2000 ppm and “off” values were positioned symmetrically to the “on” values with respect to the frequency of the  $\text{H}_2\text{O}$  (or the residual  $\text{H}_2\text{O}$ ).<sup>36</sup> Typically, 8192 or 16 284 scans were acquired. The power used for saturation transfer experiments on the Cys  $\beta$ - $\text{CH}_2$  protons was 1.8 W, applied for 5–30 ms. The other experiments were performed using power levels ranging from 0.002 to 0.2 W.

## Results

**Cu(II)–Azurin.** The  $^1\text{H}$  NMR spectrum of Cu(II)–azurin recorded at 800 MHz is reported in Figure 2A. The low molecular weight of BCPs and the high field make it possible to detect a large number of hyperfine-shifted signals with high sensitivity and resolution, since Curie relaxation<sup>51,52</sup> turns out to be negligible. Six downfield-shifted signals (A–G) are found outside the diamagnetic envelope, only one of them (signal E) being exchangeable (for evidence of the presence of signal C, see below). Two resonances were observed in the upfield region, one of them partially overlapping with the diamagnetic envelope.

**Table 1.** Assignments of the Signals Corresponding to Copper Ligands in Cu(II)– and Cu(I)–Azurin Recorded at 800 MHz, 278 K and pH 8.0

signal (OX/red)	assignment	$\delta_{\text{OX}}$ (ppm) <sup>a</sup>	$\delta_{\text{red}}$ (ppm)	$\Delta\nu_{\text{OX}}$ (Hz)
	H $\beta$ 1/2 Cys 112	850	3.48	$1.2 \times 10^6$
	H $\beta$ 2/1 Cys 112	800	2.91	$1.2 \times 10^6$
A/a	H $\delta$ 2 His 117	54.0	6.91	6000
B/b	H $\delta$ 2 His 46	49.1	5.92	5500
C/c	He1 His 117/46	46.7	6.78	
D/d	He1 His 46/117	34.1	6.87	
E'/e'	He2 His 117	27 <sup>b</sup>	11.69	
E/e	He2 His 46	26.9 <sup>b</sup>	11.46	1400
G/g	H $\alpha$ Asn 47	19.9	4.69	1200
J/j	H $\alpha$ Cys 112	–7.0	5.79	
	NH Asn 47	–30 <sup>b</sup>	10.68	

<sup>a</sup> The estimated errors are  $\pm 0.2$  ppm for signals detected directly and  $\pm 10\%$  for signals detected indirectly through saturation transfer.

<sup>b</sup> Measured in  $\text{H}_2\text{O}$ .

All of the hyperfine-shifted signals follow a Curie-temperature dependence. No other paramagnetically shifted signals could be observed beyond this spectral window. This spectrum is identical to that already reported at 600 MHz<sup>35</sup> except for the improved spectral resolution that illustrates the advantages of using high magnetic fields.

The large line widths of these signals preclude their assignment through scalar or dipolar connectivities using standard 2D techniques. However, these obstacles could be overcome by 1D or 2D saturation transfer experiments performed on a sample containing a 1:1 ratio of the oxidized and reduced species, as already done for amicyanin<sup>35</sup> and plastocyanin.<sup>36</sup> The efficiency of saturation transfer depends on the self-exchange rate between the two redox states of the protein, which, in turn, can be tuned by changing temperature and pH (as well as ionic strength). In the present case, the best conditions to achieve sizable saturation transfer were 278 K and pH 8.0, as expected from previous estimates.<sup>53</sup>

The spectrum of reduced azurin has been extensively assigned<sup>54</sup> (the assignments have been confirmed and further extended by some of us<sup>55</sup>). The saturation transfer strategy, extended to saturation of regions of the spectrum where no signal appears (e.g., 2000/100 and –10/–100 ppm), permits the identification of signals broadened beyond detection limits. In this way, we have recently identified the diamagnetic counterparts in the high-field spectrum of Cu(II)–plastocyanin, resulting in the first full assignment of the paramagnetic signals in an oxidized blue copper protein.<sup>36</sup>

Irradiation of resonances A–E yielded saturation transfer with signals in the diamagnetic envelope, as summarized in Table 1 (observation of a saturation transfer at 6.78 ppm confirms the presence of signal C). The corresponding resonances in Cu(I)–azurin are denoted with lowercase letters in Table 1. Resonance e at 11.46 ppm is well-shifted and corresponds to the signal that was not observed when the spectrum was recorded in  $\text{D}_2\text{O}$  (E), thus confirming its identity as an exchangeable imidazole proton of one of the copper-bound His. A spectrum recorded by using a 1–3–3–1 pulse sequence<sup>50</sup> allowed us to detect a signal partially overlapping with resonance E (signal E' in inset Figure 2A) that may be attributed to the exchangeable ring proton of the other copper-bound histidine.

(53) Groeneveld, C. M.; Canters, G. W. *J. Biol. Chem.* **1988**, *263*, 167–173.

(54) van de Kamp, M.; Canters, G. W.; Wijmenga, S. S.; Lommen, A.; Hilbers, C. W.; Nar, H.; Messerschmidt, A. *Biochemistry* **1992**, *31*, 10194–10207.

(55) Leckner, J. Unpublished results.

(49) Inubushi, T.; Becker, E. D. *J. Magn. Reson.* **1983**, *51*, 128–133.

(50) Hore, P. J. *J. Magn. Reson.* **1983**, *54*, 539–542.

(51) Gueron, M. *J. Magn. Reson.* **1975**, *19*, 58–66.

(52) Vega, A. J.; Fiat, D. *Mol. Phys.* **1976**, *31*, 347–355.

The corresponding signal in the reduced species ( $e'$ ) resonates at 11.69 ppm. The reported assignment of the reduced species displays the ring NH protons of His 46 and 117 at 11.59 and 11.55 ppm, respectively.<sup>54</sup> These values are too close to allow us to safely transfer the assignment to the oxidized species. However, the crystal structure of azurin reveals that His 117 is solvent-exposed;<sup>24</sup> hence its H $\epsilon$ 2 may be under a fast-exchange regime with bulk water. This behavior is also observed in solution NMR studies on Co(II)- and Ni(II)-substituted azurins.<sup>10,21,22</sup> Therefore, resonance E is attributed to the H $\epsilon$ 2 of the most buried histidine ligand, i.e., His 46.

Signals A–D correspond to the nonexchangeable H $\delta$ 2 and H $\epsilon$ 1 protons of His 46 and His 117 as it results from the observed diamagnetic shifts (cf. Table 1) and by comparison with the spectrum of Cu(II)–plastocyanin (Figure 2B). Signal B can be assigned as the H $\delta$ 2 proton of His 46, whose diamagnetic counterpart, b, exhibits a much smaller shift than the other ring protons.<sup>54,55</sup> The detailed assignment of the other three resonances is somewhat less certain, although the observed saturation transfer at 6.91, 6.78, and 6.87 ppm compares rather well with those at 6.90, 6.80, and 6.87 ppm for the reduced species, in that order.<sup>55</sup> Saturation of resonance G at 19.9 yielded a response with a diamagnetic signal located at 4.71 ppm. Among the signals around 4.71 ppm in the diamagnetic region, the only one arising from a residue that can experience a sizable hyperfine shift corresponds to the H $\alpha$  of Asn 47 (4.74 ppm).<sup>55</sup>

To identify locations of the fast-relaxing proton signals that belong to the bound Cys, we have performed a saturation transfer profile. A large spectral window was sampled following the strategy established for the study of Cu(II)–plastocyanin, as described in the Experimental Section. When the decoupler frequency was positioned in the far-downfield region, two signals experiencing saturation transfer effects at 3.48 and 2.91 ppm were detected (Figure 3A), which are assigned to cysteine  $\beta$ -CH<sub>2</sub> protons of the Cu(I) protein. Maximum saturation transfer was observed when the decoupler frequency was located between 850 and 800 ppm. We therefore assign these resonances as the cysteine  $\beta$ -CH<sub>2</sub> protons in the Cu(II) protein. The observed diamagnetic shifts are close to those already reported for the Cu(I) protein.<sup>55</sup>

Blind irradiation of the upfield region of the spectrum gave rise to a resonance at 10.68 ppm when the decoupler frequency was set at about –30 ppm. The diamagnetic value is consistent with the assignment of this resonance as the peptide NH of Asn 47, which has been located at 10.63 ppm in Cu(I)–azurin.<sup>55</sup> Irradiation at –7.5 ppm gave rise to a saturation transfer effect at 5.79 ppm, which is very close to the chemical shift value of the  $\alpha$ -CH of Cys 112 (5.74 ppm).<sup>54,55</sup> The signal I at –2.3 ppm gave a saturation transfer effect at 2.43 ppm. On the basis of our previous assignments for plastocyanin, it is reasonable to assign it to one of the  $\beta$ -CH<sub>2</sub> of His 46 that resonate, in Cu(I)–azurin, at 2.38 ppm.

**Cu(II)–Stellacyanin.** The <sup>1</sup>H NMR spectrum of Cu(II)–stellacyanin recorded at 800 MHz is reported in Figure 2C. The spectrum shows more resolved features compared to the one already reported at 500 MHz for *Rhus vernicifera* stellacyanin.<sup>16</sup> Six downfield-shifted resonances and two upfield-shifted signals were detected (the presence of signal E is ascertained through saturation transfer experiments; see below). These signals were again assigned through saturation transfer. For stellacyanin, measurable saturation transfer could be achieved at 301 K and pH 6.0. The saturation transfer pattern of signals A–D and the resulting diamagnetic shifts for the reduced protein (Table 2) are fully consistent with the assignment of these resonances as

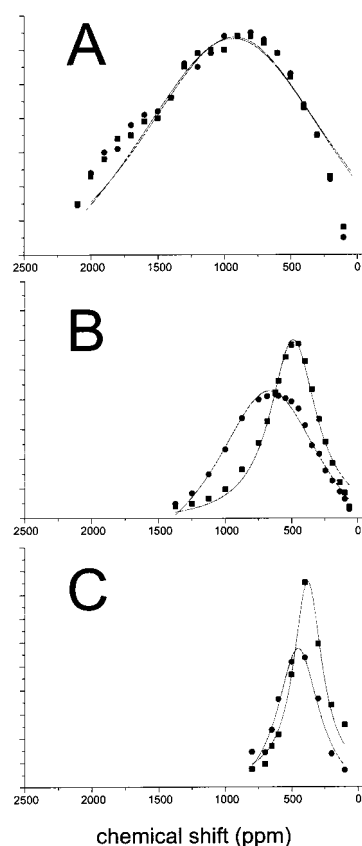


**Figure 3.** Far-downfield region of the <sup>1</sup>H NMR spectra of oxidized (A) *P. aeruginosa* azurin, (B) spinach plastocyanin, and (C) cucumber stellacyanin containing signals not observable in direct detection. The positions and line widths of the signals were obtained using saturation transfer experiments by plotting the intensity of the respective exchange connectivities with the reduced species (● indicates response from the cysteine  $\beta$ -CH<sub>2</sub> proton that resonates more downfield in the reduced species) as a function of the decoupler irradiation frequency.

**Table 2.** Assignments of the Signals Corresponding to Copper Ligands in Cu(II)– and Cu(I)–Stellacyanin Recorded at 800 MHz, 301 K and pH 6.0

signal (OX/red)	assignment	$\delta_{OX}$ (ppm) <sup>a</sup>	$\delta_{red}$ (ppm)	$\Delta\nu_{OX}$ (Hz)
	H $\beta$ 1/2 Cys 89	450	2.61	$2.8 \times 10^5$
	H $\beta$ 2/1 Cys 89	375	2.43	$2.1 \times 10^5$
A/a	H $\delta$ 2 His 94/46	55.0	7.01	3800
B/b	H $\delta$ 2 His 46/94	48.0	7.10	3000
C/c	H $\epsilon$ 1 His 94/46	41.2	7.60	3750
D/d	H $\epsilon$ 1 His 46/94	29.8	7.42	2700
E/e	H $\epsilon$ 2 His 46	26 <sup>b</sup>	10.10	
G/g	H $\alpha$ Asn 47	16.9	4.46	420
J/j	H $\alpha$ Cys 89	–7.5	5.10	
	NH Asn 47	–15 <sup>b</sup>	10.50	

<sup>a</sup> The estimated errors are  $\pm 0.2$  ppm for signals detected directly and  $\pm 10\%$  for signals detected indirectly through saturation transfer.  
<sup>b</sup> Measured in H<sub>2</sub>O.

the nonexchangeable H $\delta$ 2 and H $\epsilon$ 1 protons of His 46 and 94. In the absence of an assignment of the reduced form, the detailed assignment of these signals is only tentative and based on the analogy with plastocyanin. Irradiation of signal E yielded a saturation transfer effect with a resonance at 10.1 ppm. Following the same reasoning applied to azurin, this signal may be ascribed to the exchangeable H $\epsilon$ 2 proton of the most buried histidine, His 46. The corresponding resonance of His 94 was not detected. This is attributable to the larger degree of solvent exposure of the active site in stellacyanin, as shown in previous NMR

experiments in the Co(II)-substituted protein<sup>12</sup> and later confirmed by the crystallographic structure.<sup>29</sup>

The Cys signals were also localized by performing the blind saturation transfer profile (Figure 3C). As shown in the corresponding figure, the  $\beta$ -CH<sub>2</sub> Cys protons were found at 375 and 450 ppm. The resulting saturation transfer profile (Figure 3C) reveals a significant sharpening of these signals compared to those obtained for azurin and plastocyanin. When signal J (at -7.5 ppm) was irradiated, saturation transfer was observed with a resonance at 5.10 ppm. We therefore assigned signal J as the  $\alpha$ -CH proton of Cys 89.

Signal G displayed a saturation transfer with a resonance located at 4.46 ppm, indicating that it may presumably be the H $\alpha$  of Asn 47. The corresponding NH proton was found at -15 ppm through blind irradiation in the upfield region, with a corresponding diamagnetic shift of 10.50 ppm. The other resolved upfield signal (I) was connected to a resonance at 2.6 ppm. We tentatively assign signal I as a  $\beta$ -CH<sub>2</sub> of one of the bound histidines.

At this stage, an extensive assignment of the hyperfine-shifted signals for azurin and stellacyanin is obtained which adds to the analogous analyses of plastocyanin.<sup>36</sup> It is definitely shown that the <sup>1</sup>H NMR investigation of oxidized BCPs is feasible. Therefore, the strategy of investigation of oxidized BCPs is definitely outlined after the pioneering work of Canters in 1996.<sup>35</sup>

## Discussion

**Analysis of the Isotropic Shifts.** We succeeded in assigning the hyperfine-shifted resonances in the oxidized species of azurin and stellacyanin. This was made possible by the observation of saturation transfer due to favorable electron self-exchange rates. For stellacyanin, the pH and the temperature conditions were analogous to those for plastocyanin, while higher pH and lower temperatures were needed to slow the electron self-exchange rates of azurin to the proper values. The faster electron self-exchange rates in azurin can be ascribed to its smaller overall charge with respect to the other two proteins.<sup>53,56</sup> The availability of these assignments, together with those earlier obtained for Cu(II)-plastocyanin,<sup>36</sup> allows us to perform a detailed comparison of the spectral features of this series of BCPs.

The isotropic shifts in paramagnetic systems are the result of three terms:<sup>57</sup>

$$\delta_{\text{obs}} = \delta_{\text{dia}} + \delta_{\text{con}} + \delta_{\text{pc}} \quad (1)$$

where  $\delta_{\text{obs}}$  is the experimental shift,  $\delta_{\text{dia}}$  is the chemical shift of the nucleus in an analogous diamagnetic system,  $\delta_{\text{con}}$  is the Fermi contact shift due to the unpaired electron density on the nucleus of interest arising from electron delocalization,<sup>58,59</sup> and  $\delta_{\text{pc}}$  represents the pseudocontact shift stemming from the magnetic anisotropy of the unpaired electron residing on the metal ion.<sup>59,60</sup> In the present case,  $\delta_{\text{dia}}$  corresponds to the chemical shift in the respective Cu(I) protein that is directly measured in the saturation transfer experiment under the same experimental conditions in which  $\delta_{\text{obs}}$  is retrieved.

(56) Kyritsis, P.; Dennison, C.; Ingledew, W. J.; McFarlane, W.; Sykes, A. G. *Inorg. Chem.* **1995**, *34*, 5370–5374.

(57) Bertini, I.; Luchinat, C. *NMR of paramagnetic substances*; Coordination Chemistry Review 150; Elsevier: Amsterdam, 1996; pp 1–300.

(58) McConnell, H. M.; Chesnut, D. B. *J. Chem. Phys.* **1958**, *28*, 107–117.

(59) Kurland, R. J.; McGarvey, B. R. *J. Magn. Reson.* **1970**, *2*, 286–301.

(60) McConnell, H. M.; Robertson, R. E. *J. Chem. Phys.* **1958**, *29*, 1361–1365.

The pseudocontact contribution can be calculated using information derived from the protein structure and available magnetic susceptibility anisotropy tensor, or from the **g** tensor (whose square is proportional to the  $\chi$  tensor for  $S = 1/2$  systems with a well-isolated orbitally nondegenerate ground state).<sup>57</sup> The **g** tensor for azurin displays a small rhombicity when determined at high-field EPR ( $g_{yy} - g_{xx} = 0.0175$ ), which we consider to be negligible for our calculations.<sup>61,62</sup> The  $z$ -axis makes an angle of 15° with the Cu–S $\delta$ (Met121) bond, whereas the ( $x, y$ ) axes are approximately parallel to the NNS plane determined by the equatorial ligands, with the  $y$  axis making an angle of 24° with the Cu–S $\gamma$ (Cys112) bond.<sup>61</sup> The principal directions of the **g** tensor for stellacyanin are not currently available. Therefore, we used data from Met121Gln azurin mutant, which mimics the electronic structure of the copper site in stellacyanin.<sup>63</sup> In this mutant, the magnetic  $z$  axis is tilted 10° with respect to the Cu–O $\epsilon$ (Gln121) bond, whereas the ( $x, y$ ) axes are rotated by  $\sim 30^\circ$  with respect to the orientation found in wild-type azurin.<sup>64</sup> Although the rhombicity in stellacyanin is larger ( $g_{yy} - g_{xx} = 0.052$ ),<sup>48</sup> it still remains negligible for the present calculations. By assuming axial **g** tensors for both proteins, defined by  $g_{\parallel} = g_{zz}$  and  $g_{\perp} = (g_{xx} - g_{yy})/2$ , the following equation may be used to calculate the pseudocontact contribution to the observed shifts:<sup>59,60</sup>

$$\delta_{\text{pc}} = \frac{\mu_0 \mu_B^2 S(S+1)}{4\pi 9kTr^3} (3 \cos^2 \theta - 1) (g_{\parallel}^2 - g_{\perp}^2) \times 10^6 \quad (2)$$

where  $\mu_0$  is the magnetic permeability in vacuum,  $\mu_B$  is the electron Bohr magneton,  $k$  is Boltzmann's constant,  $T$  is the absolute temperature,  $r$  is the proton–copper distance, and  $\theta$  is the angle between the metal–proton vector and the magnetic  $z$  axis. Even though there is a nonnegligible unpaired electron density on the sulfur atom, we have calculated the pseudocontact shift based on the metal-centered approximation.

Table 3 reports the structural parameters together with the pseudocontact contributions of each nucleus, which in fact, are small compared to the measured shifts, clearly dominated by the Fermi contact contribution (also reported in Table 3). From these values, the hyperfine coupling constants for each nuclei ( $A/h$ ) may be calculated from the following equation:<sup>58,59</sup>

$$\frac{A}{h} = \frac{1}{2\pi} \frac{\delta_{\text{con}} 3\gamma_N kT}{g_{\text{av}} \mu_B S(S+1)} \quad (3)$$

where  $\gamma_N$  is the nuclear magnetogyric ratio and  $g_{\text{av}}$  is the average  $g$  value. The resulting hyperfine coupling constants are listed in Table 4 together with those of plastocyanin for comparison purposes. We will now analyze the results by examining the changes in the different ligands.

**The Cysteine Signals.** The most notable features of the present NMR spectra are the large hyperfine coupling constants observed for the  $\beta$ -CH<sub>2</sub> Cys protons. This observation is in agreement with results obtained from different spectroscopic

(61) Coremans, J. W. A.; Poluektov, O. G.; Groenen, E. J. J.; Canters, G. W.; Nar, H.; Messerschmidt, A. *J. Am. Chem. Soc.* **1996**, *118*, 12141–12153.

(62) Coremans, J. W. A.; Poluektov, O. G.; Groenen, E. J. J.; Canters, G. W.; Nar, H.; Messerschmidt, A. *J. Am. Chem. Soc.* **1997**, *119*, 4726–4731.

(63) Romero, A.; Hoitink, C. W. G.; Nar, H.; Huber, R.; Messerschmidt, A.; Canters, G. W. *J. Mol. Biol.* **1993**, *229*, 1007–1021.

(64) Coremans, J. W. A.; Poluektov, O. G.; Groenen, E. J. J.; Warmerdam, G. C. M.; Canters, G. W.; Nar, H.; Messerschmidt, A. *J. Phys. Chem.* **1996**, *100*, 19706–19713.

**Table 3.** Separation of the Hyperfine Shifts for Cu(II)–Azurin and –Stellacyanin

	$\theta^a$	$r_{\text{Cu-H}}^a$	$\delta_{\text{obs}}$ (ppm)	$\delta_{\text{dia}}$ (ppm)	$\delta_{\text{pc}}$ (ppm)	$\delta_{\text{con}}$ (ppm)
Azurin						
H $\beta$ 1 Cys 112	64.1	3.48	850/800	3.48/2.91	-1.8	~850/800
H $\beta$ 2 Cys 112	55.9	3.36	800/850	2.91/3.48	-0.3	~800/850
H $\delta$ 2 His 117	80.5	5.20	54.0	6.91	-1.1	48.2
H $\delta$ 2 His 46	94.4	5.11	49.1	5.92	-1.3	44.5
He1 His 117	109.3	3.25	46.7/34.1	6.78/6.87	-3.4	43.3/30.6
He1 His 46	74.5	3.12	34.1/46.7	6.87/6.78	-4.5	31.7/44.4
He2 His 46	83.0	4.98	26.9	11.46	-1.3	16.7
H $\alpha$ Asn 47	114.7	6.66	19.9	4.71	-0.3	15.5
H $\alpha$ Cys 112	84.1	5.10	-7.0	5.79	-1.3	-11.5
NH Asn 47	112.7	4.04	-30	10.68	-1.5	~-39
Stellacyanin						
H $\beta$ 1 Cys 89	59.1	3.33	450/375	2.61/2.43	-1.0	~450/375
H $\beta$ 2 Cys 89	51.5	3.27	375/450	2.43/2.61	0.8	~370/450
H $\delta$ 2 His 94	107.5	5.07	55.0/48.0	7.01/7.10	-1.0	49.0/41.9
H $\delta$ 2 His 46	86.1	5.06	48.0/55.0	7.10/7.01	-1.3	42.2/49.3
He1 His 94	136.2	3.12	41.2/29.8	7.60/7.42	-5.4	39.0/27.8
He1 His 46	83.4	3.12	29.8/41.2	7.42/7.60	3.1	19.3/30.5
He2 His 46	84.0	4.93	26	10.10	-1.4	~17
H $\alpha$ Asn 47	97.6	6.52	16.9	4.46	-0.6	13.04
H $\alpha$ Cys 89	77.3	4.99	-7.5	5.10	-1.2	-11.4
NH Asn 47	96.7	3.78	-15	10.50	-3.0	~-22

<sup>a</sup> From pdb files 4azu (azurin) and 1jer (stellacyanin).

**Table 4.** Hyperfine Coupling Constants in Azurin, Plastocyanin, and Stellacyanin

azurin		plastocyanin		stellacyanin	
residue	A/h (MHz)	residue	A/h (MHz)	residue	A/h (MHz)
H $\beta$ 1 Cys 112	28/27	H $\beta$ 1 Cys 84	23	H $\beta$ 1 Cys 89	16/13
H $\beta$ 2 Cys 112	27/28	H $\beta$ 2 Cys 84	17	H $\beta$ 2 Cys 89	13/16
H $\alpha$ Cys 112	-0.38	H $\alpha$ Cys 84	-0.44	H $\alpha$ Cys 89	-0.41
H $\delta$ 2 His 117	1.61	H $\delta$ 2 His 87	1.63	H $\delta$ 2 His 94	1.77/1.51
H $\delta$ 2 His 46	1.49	H $\delta$ 2 His 37	1.45	H $\delta$ 2 His 46	1.53/1.78
He1 His 117	1.45/1.02	He1 His 87	1.01	He1 His 94	1.40/1.01
He1 His 46	1.06/1.48	He1 His 37	1.14	He1 His 46	0.70/1.09
He2 His 46	0.56	He2 His 37	0.74	He2 His 46	0.62
H $\alpha$ Asn 47	0.52	H $\alpha$ Asn 38	0.47	H $\alpha$ Asn 47	0.47
NH Asn 47	-1.3	NH Asn 38	-1.0	NH Asn 47	-0.8

techniques,<sup>42,45</sup> in that it confirms that one of the distinctive features of BCPs in their oxidized state is the strong covalency of the Cu(II)–Cys bond (cf. Table 5). The large predominance of the contact contribution to the experimental shift makes this technique appealing for a direct characterization of the Cu(II)–Cys bonding. In addition, it is remarkable that these shifts display ample variations among the different proteins examined, ranging from 850 to 375 ppm.

The H $\alpha$  Cys displays a negative hyperfine coupling constant in all three BCPs, indicating a similar spin polarization mechanism operative in the Cys moiety through the  $\pi$  sulfur orbital which contributes to the HOMO. This view is supported by the alternating sign of the hyperfine coupling constant in the conserved Asn residue that is hydrogen bonded to the Cys sulfur (cf. Tables 1 and 2).<sup>24,29</sup> Hence, the electron delocalization onto the H $\alpha$  does not differ considerably among the different proteins notwithstanding the distinct shifts in the vicinal  $\beta$ -CH<sub>2</sub> moiety. This is consistent with the large attenuation of the electron delocalization existing in saturated carbon skeletons.<sup>57</sup> On the other hand, the amide NH from the Asn residue, which is hydrogen bonded to the sulfur Cys, exhibits the same qualitative trend observed for the  $\beta$ -CH<sub>2</sub> Cys protons. A net contact interaction in the amide proton of the hydrogen Asn

residue is found in all the studied BCPs, and it was also found in cobalt(II)–azurin.<sup>18</sup>

The hyperfine coupling constants of the Cys  $\beta$ -CH<sub>2</sub> protons are proportional to the electron spin density on the 1s orbitals of these nuclei. In the absence of a spin-polarization mechanism, the spin density would coincide with the fraction of delocalized unpaired electron on the sulfur atom. The overlap between the sulfur p $\pi$  orbital and the metal orbital containing the unpaired electron<sup>41</sup> is a mechanism that contributes to the spin density on  $\beta$ -protons through a sine-squared dependence of the M–S–C–H dihedral angle.<sup>65</sup> Indeed, the hyperfine shifts follow a sine-squared dependence on the above angle.<sup>36</sup> When nitrogen is a donor atom, the dependence is of a cosine-squared type.<sup>66</sup> In principle, a mixed dependence on both  $\sigma$  and  $\pi$  spin delocalization mechanisms may be operative.<sup>65</sup>

The hyperfine coupling constants in stellacyanin are decreased by ~30% with respect to plastocyanin. The present results closely parallel the electron occupancy changes predicted by SCF-X $\alpha$  SW calculations for the non-sulfur Cys atoms.<sup>67</sup> The stronger interaction of the copper(II) with the axial Gln in stellacyanin (Table 5) imposes a tetrahedral distortion to the site (Figure 1),<sup>29,67</sup> which finally weakens the copper(II)–Cys bond. XAS<sup>67</sup> (Table 5) and resonance Raman<sup>68</sup> on the Cu(II) protein, as well as NMR data on the cobalt(II) derivative<sup>11,12</sup> also support this view.

Azurin exhibits the largest hyperfine coupling onto the Cys protons among the examined proteins. By extrapolating the data on stellacyanin and plastocyanin, we can state that azurin exhibits the highest degree of Cu(II)–Cys covalency in the whole series. This observation is in line with the crystal structure of azurin.<sup>24</sup> The Cu(II) ion is coplanar with the His<sub>2</sub>Cys ligand donor set, the axial ligands (Met 121 and Gly 45) being both at a distance larger than 3.0 Å from the metal (Table 5). The presence of two weak binding, counterbalancing axial ligands at both sides of the ligand set plane may seem to force the metal ion to lie in the plane (Figure 1). This coplanarity finally results in an enhancement of the Cu(II)–Cys covalency.

The overall view provided by the present NMR data fits nicely with the picture of metal–ligand bonding in BCPs.<sup>30,37,43,46</sup> This is not the case, however, if the hyperfine coupling constants from ENDOR experiments are considered (Table 5).<sup>45</sup> Not only do the ENDOR values differ from the present NMR data, but no general trends can be retrieved from them. These differences could be attributed to the conditions in which the ENDOR experiments are normally performed, i.e., frozen samples at cryogenic temperatures. Some changes attributable to the freezing procedure may be responsible for these differences.

**The Histidine Signals.** The His signal pattern is conserved in the three studied proteins, with the following trend in the contact shifts: H $\delta$ 2 > He1 > He2, indicating the existence of a similar delocalization mechanism in all these imidazole rings. The hyperfine coupling constants of the H $\delta$ 2 protons of both His are comparable in the three proteins, the larger shift being experienced by the downstream histidine. This is in agreement with ESEEM<sup>61,62,69</sup> and ENDOR<sup>45</sup> data.

(65) Bertini, I.; Capozzi, F.; Luchinat, C.; Piccioli, M.; Vila, A. J. *J. Am. Chem. Soc.* **1994**, *116*, 651–660.

(66) Ho, F. F. L.; Reilly, C. N. *Anal. Chem.* **1969**, *41*, 1835–1841.

(67) LaCroix, L. B.; Randall, D. W.; Nersissian, A. M.; Hoitink, C. W. G.; Canters, G. W.; Valentine, J. S.; Solomon, E. I. *J. Am. Chem. Soc.* **1998**, *120*, 9621–9631.

(68) Blair, D. F.; Campbell, G. W.; Schoonover, J. R.; Chan, S. I.; Gray, H. B.; Malmström, B. G.; Pecht, I.; Swanson, B. I.; Woodruff, W. H.; Cho, W. K.; English, A. M.; Fry, H. A.; Lum, V.; Norton, K. A. *J. Am. Chem. Soc.* **1985**, *107*, 5755–5766.

(69) Bender, C. J.; Peisach, J. *J. Chem. Soc., Faraday Trans.* **1998**, *94*, 375–386.

**Table 5.** Spectral Properties of Azurin, Plastocyanin, and Stellacyanin

$A/h$ (NMR) <sup>a</sup>	unpaired spin density on $\beta$ -CH <sub>2</sub> <sup>a</sup> (%)	$A/h$ (ENDOR) <sup>b</sup>	HOMO-S covalency (XAS) <sup>c</sup>	total oscillator strength Cys LMCTs <sup>c</sup>	$r_{\text{Cu-X}}$ (donor atom-axial ligand)
Azurin					
28	2.0	23	nd <sup>d</sup>	nd <sup>d</sup>	3.1 (S $\delta$ -Met) <sup>24</sup>
27	1.9	18			
Plastocyanin					
23	1.6	27	38%	0.0544	2.8 (S $\delta$ -Met) <sup>27</sup>
17	1.2	16			
Stellacyanin					
16	1.1	20	24%	0.0513	2.2 (O $\epsilon$ -Gln) <sup>29</sup>
13	0.9	20			

<sup>a</sup> This work. <sup>b</sup> From ref 45. <sup>c</sup> From ref 67. <sup>d</sup> nd, not detected.

**The Axial Ligand.** The most striking difference between the spectra of the present proteins, i.e., stellacyanin and azurin, when compared to the recently assigned spectrum of plastocyanin, is the absence of isotropically shifted signals attributable to the axial ligands (Met-Gly for azurin, and Gln for stellacyanin). This situation is not unreasonable for azurin, since the S $\delta$ -Met 121 and, even more, the peptidic O from Gly 45 are at a relatively long distance from the metal. By these means, it can be clearly stated that, in azurin, the Cu-S $\delta$ (Met) bond must have very little bonding character.

The situation is less straightforward in stellacyanin, since the weakening of the Cu(II)-Cys covalency was generically associated with a stronger interaction with the axial ligand,<sup>29</sup> as in the azurin Met121Gln mutant.<sup>63</sup> This interaction occurs, in fact, according to the shorter Cu-O $\epsilon$  Gln 99 distance in stellacyanin,<sup>29</sup> but the unpaired electron spin density on the  $\gamma$ -CH<sub>2</sub> protons seems to be small, according to the lack of substantial Fermi contact shifts. There are two possible rationales for this fact. The  $\gamma$ -CH<sub>2</sub> geminal couple is four bonds away from the metal ion, whereas the equivalent protons in a coordinated Met residue (such as in plastocyanin) are only three bonds away from the Cu(II). If the attenuation of the electron spin delocalization in the axial ligand within an alkyl chain is as large as in the Cys residue, a strong contact interaction should not be expected for these protons. The same holds for the terminal amide protons of the Gln residue. On the other hand, we should consider that a recent study revealed that no LMCT transitions from the axial Gln were present in the electronic spectrum of stellacyanin, this being consistent with a null contribution of this residue to the HOMO, in which the unpaired electron is located.<sup>67</sup> Instead, in plastocyanin, Met-Cu(II) LMCT bands were identified, as well as a net contribution of the Met orbitals into the HOMO, being consistent with the finding of net unpaired electron density in Met 92.<sup>40,41</sup>

**Nuclear Relaxation Features.** Inspection of the spectra reported in Figure 2 shows that the hyperfine-shifted signals of the three BCPs display different line widths. As already discussed,<sup>36</sup> the line widths in these systems are determined by dipolar and contact contributions. The former depend on the reciprocal sixth power of the metal-nucleus distance, while the latter depend on the square of the hyperfine coupling constant, which in turn is proportional to the contact shift. Indeed, it was observed<sup>36</sup> that the line widths of some signals (e.g., the  $\beta$ CH<sub>2</sub> protons of the bound cysteine) are dominated by contact relaxation while some others (e.g., the bound His H $\epsilon$ 1 signals) are dominated by dipolar relaxation. In any case, both dipolar and contact contributions are proportional to the electron

longitudinal relaxation time  $\tau_s$ . For signals with similar hyperfine shifts arising from protons at similar distance from the metal ion in the three proteins, the line widths should hold the same ratio as the  $\tau_s$  values. According to this reasoning, and referring to the histidine H $\delta$ 2 protons, we can qualitatively state that  $\tau_s$  is the shortest for plastocyanin. It then should be slightly longer in stellacyanin and  $\sim$ 2 times longer in azurin. For azurin, a value of 0.8 ns was estimated.<sup>33</sup>

### Concluding Remarks

The <sup>1</sup>H NMR spectra of the ligands of copper(II) proteins are hard to detect due to the long electronic relaxation time of the unpaired electron, that is the correlation time for the electron-nucleus interaction. However, it has been shown that BCPs are the least unfavorable among copper(II) proteins for NMR spectroscopy.

We have been able to observe the  $\beta$ -CH<sub>2</sub> signals of the coordinated cysteines in both azurin and stellacyanin, although these resonances are broad beyond detectable limits using direct detection. This allowed us to carry out an extensive assignment of the hyperfine-shifted signals belonging to the copper(II) ligands and to perform an instructive comparison with plastocyanin. The shifts of the Cys  $\beta$ -CH<sub>2</sub>'s largely vary among the different proteins, ranging from 375 to 850 ppm. Such values have been related to the strength of the axial ligand(s) and to the planarity of the Cu(II)-N(His)<sub>2</sub>S(Cys) moiety. The  $\beta$ -CH<sub>2</sub> Cys shifts are proposed to depend on the overlap of the 1s orbital of H and p $\pi$  orbital of S according to the electronic structure described by Solomon and co-workers.<sup>40,41</sup> We can state at this point that NMR is a useful tool to monitor the structure around copper(II) and some electronic properties such as spin delocalization and spin relaxation. It seems that the study of the structure in solution and of the mobility of BCPs is from now on possible.

**Acknowledgment.** C.O.F. thanks Fundacion Antorchas and ANPCYT for financial support and the University of Buenos Aires for a travel grant. Work at UCLA was supported by NIH Grant GM-28222 to J.S.V. Work at the University of Florence was supported by MURST, funding program ex-40% 1997, CNR Contract 98.01789.CT03, and EU RTD project "Development of large bandwidth and dipolar coupling probes" Contract ERB FMGECT980107. B.G.K., J.L., and B.G.M. acknowledge the support from the Florence Large Scale Facility PARABIO under EU Contract ERB FMGECT950033.

JA992674J